

# Extended Shell Model Calculation for even $N = 82$ Isotones with a Realistic Effective Interaction

A. Holt, T. Engeland and E. Osnes

*Department of Physics, University of Oslo, N-0316 Oslo, Norway*

M. Hjorth-Jensen

*Nordita, Blegdamsvej 17, DK-2100 København Ø, Denmark*

J. Suhonen

*Department of Physics, University of Jyväskylä, P.O.Box 35, FIN-40351 Jyväskylä, Finland*

**Abstract:** The shell model within the  $2s1d0g_{7/2}0h_{11/2}$  shell is applied to calculate nuclear structure properties of the even  $Z = 52 - 62$ ,  $N = 82$  isotones. The results are compared with experimental data and with the results of a quasiparticle random-phase approximation (QRPA) calculation. The interaction used in these calculations is a realistic two-body  $G$ -matrix interaction derived from modern meson-exchange potential models for the nucleon-nucleon interaction. For the shell model all the two-body matrix elements are renormalized by the  $\hat{Q}$ -box method whereas for the QRPA the effective interaction is defined by the  $G$ -matrix.

## 1 Introduction

In recent years the  $N = 82$  isotones have been a subject of great interest and experimental data for the isotones are rather well established. These nuclei show a high degree of regularity, in the sense that there are many similarities between

*To appear in Physics Reports (1995)*

neighbouring even-even nuclei. Abbas [1] even goes as far as to claim that all the  $N = 82$  and  $Z = 58, 60, 62, 64, 66, 68, 70$  nuclei were doubly magic. At least for  $^{146}\text{Gd}$  the doubly magic character and the subshell closure at  $Z = 64$  is rather well established [2,3].

During the last few years experimental evidence for low-lying octupole-octupole and octupole-quadrupole multiplets has been reported for the semi-magic  $N = 82$  isotones [4–7]. These are states built on  $3^-$  collective octupole vibrational states. However, most of the low-lying states of these isotones can be interpreted as pure excitations of valence protons outside a  $^{132}\text{Sn}$  closed core, and it offers a unique opportunity for studying the microscopic foundation of various nuclear models.

Systematic studies of the  $N = 82$  isotones have been carried out by Andreozzi *et al.* [8] who investigated the importance of pairing effects in these nuclei. Scholten *et al.* [9–11] have also studied the  $N = 82$  isotones and compared the generalized seniority scheme with the shell model. The most comprehensive shell model study, up to now, was carried out by Wildenthal [12] for the  $N = 82$  isotones ranging from  $^{133}\text{Sb}$  to  $^{154}\text{Hf}$ . The dimension of the problem was however reduced by both an occupation number and a seniority truncation. The effective two-body forces used in the above-mentioned shell model calculations are all rather schematic, phenomenological interactions.

One aim of this work is to calculate an effective interaction based on modern meson-exchange models for the nucleon-nucleon (NN) potential. The first step in the derivation of an effective interaction  $V_{\text{eff}}$  is to renormalize the NN potential through the so-called  $G$ -matrix. The  $G$ -matrix is in turn used in a perturbative many-body scheme discussed in Sect. 2 to derive an effective interaction for the  $N = 82$  isotones.

The second aim is to use this effective interaction in a full shell model (SM) calculation, within a model space or  $P$ -space consisting of the orbitals  $2s_{1/2}$ ,  $1d_{5/2}$ ,  $1d_{3/2}$ ,  $0g_{7/2}$  and  $0h_{11/2}$  for the  $Z = 52 - 64$ ,  $N = 82$  isotones. This is the first time that a full shell model calculation without any truncations has been performed for these nuclei.

We have performed two similar and quite extended shell model calculations for the Sn isotopes, one having the doubly magic  $^{100}\text{Sn}$  as a closed core [13], and the other having the doubly magic  $^{132}\text{Sn}$  as a closed core [14]. In the former, valence neutron particles have been added to the  $^{100}\text{Sn}$  core, and in the latter valence neutron particles have been subtracted from (or in other words, neutron holes have been added to) the  $^{132}\text{Sn}$  core. In this work we present a further test of our method in the region of medium-heavy nuclei. In our previous works on the Sn isotopes, we have carried out calculations based on the neutron-neutron particle

interaction and the neutron-neutron hole interaction, respectively. In the present case an analogous test of the proton-proton particle interaction is provided by the  $N = 82$  isotones.

Our third aim is to compare the shell model results with results from a quasi-particle random-phase approximation (QRPA) calculation. We are performing the comparison with QRPA in order to test the perturbation technique and to study to what extent the effective matrix elements give satisfactory results. For the QRPA we take as effective interaction the same  $G$ -matrix as the one used in the perturbative many-body scheme discussed above, but the model space is enlarged by including the  $1p0f$  shell as well.

The philosophy behind the perturbative approach is to include degrees of freedom not accounted for in the model space through various terms in perturbation theory. Therefore, since the QRPA calculation discussed here employs a larger single-particle space than the perturbative many-body scheme, the hope is that the two approaches can shed light on different many-body contributions and their influence on various spectroscopic observables.

This work is organized as follows: In Sect. 2 we give a brief sketch on how to derive the effective interaction. In the subsequent section some general spectroscopic features about the  $N = 82$  isotones are given together with a description of the shell model problem. In Sect. 4, a short overview of the QRPA relevant for the  $N = 82$  isotones is given, whereas our results and discussions are presented in Sect. 5. Concluding remarks are drawn in Sect. 6.

## 2 Effective interaction for the $N = 82$ isotones

In nuclear structure calculations, we solve the quantum many-body Schrödinger equation for an  $A$ -nucleon system

$$H\Psi_i(1, \dots, A) = E_i\Psi_i(1, \dots, A) \quad (1)$$

in a restricted Hilbert space, referred to as the model space. In Eq. (1), we have defined  $H = T + V$ ,  $T$  being the kinetic energy operator and  $V$  the nucleon-nucleon (NN) potential.  $E_i$  and  $\Psi_i$  are the eigenvalues and eigenfunctions for a state  $i$  in the Hilbert space. Introducing the auxiliary single-particle potential  $U$ ,  $H$  can be rewritten as

$$H = H_0 + H_1; H_0 = T + U; H_1 = V - U. \quad (2)$$

If  $U$  is chosen such that  $H_1$  becomes small, then  $H_1$  can be treated as a perturbation. The eigenfunctions of  $H_0$  are then the unperturbed wave functions  $\psi_i$ . These eigenfunctions can, in turn, be used to define a projection operator for the above-mentioned model space

$$P = \sum_{i=1}^d |\psi_i\rangle \langle \psi_i|, \quad (3)$$

with  $d$  being the size of the model space, and an excluded space defined by the operator  $Q$

$$Q = \sum_{i=d+1}^{\infty} |\psi_i\rangle \langle \psi_i|, \quad (4)$$

such that  $PQ = 0$ . The assumption then is that the most relevant components of the low-lying nuclear states can be fairly well reproduced by configurations consisting of few particles and holes occupying a limited number of orbitals  $\psi_i$  selected on physical grounds. These selected orbitals define the model space.

Eq. (1) can be rewritten as a secular equation

$$PH_{\text{eff}}P\Psi_i = P(H_0 + V_{\text{eff}})P\Psi_i = E_iP\Psi_i, \quad (5)$$

where  $H_{\text{eff}}$  now is an effective hamiltonian acting solely within the chosen model space. The definition of this effective interaction is that it should act within the chosen model space and that the model-space eigenvalue problem yields some of the eigenvalues of the original hamiltonian. In general, however, these requirements do not determine the effective interaction uniquely, as discussed in Refs. [15–18]. Several many-body techniques exist for deriving the effective interaction [15,17,18]. In this work we shall derive the effective interaction using a time-dependent approach, starting from the time evolution operator  $U(t, t')$  [16]. Our effective interaction is derived by the so-called folded-diagram expansion method of Kuo and co-workers [16] (see below). The folded diagrams represent a set of diagrams which can be summed to infinite order through e.g. iterative methods. They arise when one removes the dependence on the exact energy of the perturbation expansion.

Our scheme to obtain an effective interaction, appropriate for the  $N = 82$  isotones, starts with  $A = 132$  as the closed-shell core, and can be divided into three steps. A more detailed exposition can be found in Ref. [15].

First, one needs a free NN interaction  $V$  which is appropriate for nuclear physics at low and intermediate energies. At present, a meson-exchange picture for the potential model seems to offer a viable approach. Among such meson-exchange models, one of the most successful is the one-boson-exchange model of the Bonn

group [19]. As a starting point for our perturbative analysis, we shall use the parameters of the Bonn A potential defined in table A.1 of Ref. [19]. For applications of this potential to nuclear structure, see e.g., Ref. [19].

In nuclear many-body calculations the first problem one is confronted with is the fact that the repulsive core of the NN potential  $V$  is unsuitable for perturbative approaches. This problem is overcome by the next step in our many-body scheme, namely by introducing the reaction matrix  $G$

$$G = V + V \frac{\tilde{Q}}{\omega - H_0} G, \quad (6)$$

where  $\omega$  is the unperturbed energy of the interacting nucleons, and  $H_0$  is the unperturbed hamiltonian. The operator  $\tilde{Q}$ , commonly referred to as the Pauli operator, is a projection operator which prevents the interacting nucleons from scattering into states occupied by other nucleons. In this work we solve the Bethe-Goldstone equation, using the so-called double-partitioning scheme [15], replacing  $H_0$  in the denominator of Eq. (6) by  $\tilde{Q}T\tilde{Q}$ . To construct the Pauli operator which defines  $G$ , one has to take into account that neutrons and protons have different closed shell cores,  $N = 82$  and  $Z = 50$ , respectively. This means that neutrons in the  $2s1d0g_{7/2}0h_{11/2}$  shell are holes, while protons in the  $2s1d0g_{7/2}0h_{11/2}$  shell are particles. For protons the Pauli operator must be constructed so as to prevent scattering into intermediate states with a single proton in any of the states defined by the orbitals from the  $0s$  shell up to the  $0g_{9/2}$  orbital. For a two-particle state with protons only, one has also to avoid scattering into states with two protons in the  $2s1d0g$  ( $0g_{9/2}$  excluded) and the  $2p1f0h$  shells. For neutrons one must prevent scattering into intermediate states with a single neutron in the orbitals from the  $0s$  shell up to the  $0h_{11/2}$  orbital. In addition, in case of a two-particle state with neutrons only, one must prevent scattering into states with two neutrons in the  $0h_{9/2}0i_{13/2}1f2p$  shell and the  $3s2d1g0i_{11/2}0j_{15/2}$  shell. If we have a proton-neutron two-particle state we must in addition prevent scattering into two-body states where a proton is in the  $2s1d0g$ - ( $0g_{9/2}$  excluded) and the  $2p1f0h$  shells and a neutron is in the  $0h_{9/2}0i_{13/2}1f2p$  shell and the  $3s2d1g0i_{11/2}0j_{15/2}$  shell. The single-particle wave functions were chosen to be harmonic oscillator eigenstates with the oscillator energy  $\hbar\Omega = 45A^{-1/3} - 25A^{-2/3} = 7.87$  MeV, for  $A = 132$ . This  $G$ -matrix will also be used as the effective interaction in the QRPA calculations discussed in the next section.

The last step consists in defining a two-body interaction in terms of the  $G$ -matrix. The first step here is to define the so-called  $\hat{Q}$ -box given by

$$P\hat{Q}P = PH_1P + P \left( H_1 \frac{Q}{\omega - H_0} H_1 + H_1 \frac{Q}{\omega - H_0} H_1 \frac{Q}{\omega - H_0} H_1 + \dots \right) P, \quad (7)$$

where we will replace  $H_1$  with  $G - U$  ( $G$  replaces the free NN interaction  $V$ ). The  $\hat{Q}$ -box is made up of non-folded diagrams which are irreducible and valence linked. A diagram is said to be irreducible if between each pair of vertices there is at least one hole state or a particle state outside the model space. In a valence-linked diagram the interactions are linked (via fermion lines) to at least one valence line. Note that a valence-linked diagram can be either connected (consisting of a single piece) or disconnected. In the final expansion, including folded diagrams as well, the disconnected diagrams are found to cancel out [16]. This corresponds to the cancellation of unlinked diagrams of the Goldstone expansion [16]. The projection operator  $Q$  used in the definition of the effective interaction need not be the same as  $\hat{Q}$  used in the calculation of the  $G$ -matrix. This is the case in our calculation since we are using the double-partitioning scheme for calculating the  $G$ -matrix. Such an approach leads to the inclusion of additional ladder diagrams in the definition of the  $\hat{Q}$ -box, as discussed in Ref. [15]. We obtain the effective interaction,  $H_{\text{eff}} = H_0 + V_{\text{eff}}$ , in terms of the  $\hat{Q}$ -box as [15,16]

$$V_{\text{eff}}^{(n)} = \hat{Q} + \sum_{m=1}^{\infty} \frac{1}{m!} \frac{d^m \hat{Q}}{d\omega^m} \{V_{\text{eff}}^{(n-1)}\}^m. \quad (8)$$

Observe also that the effective interaction  $V_{\text{eff}}^{(n)}$  is evaluated at a given model space energy  $\omega$ , as is the case of the  $G$ -matrix. Here we choose  $\omega = -20$  MeV, although the dependence of the final resulting spectra of the choice of starting energy is rather weak. Since the higher-order derivatives of the  $\hat{Q}$ -box are rather small, the series can be truncated at  $m \sim 6 - 10$ , and similarly some 6 - 10 iterations  $n$  are needed for convergence of the effective interaction. The  $\hat{Q}$ -box in this work is defined to be the sum of all non-folded diagrams through third order in the  $G$ -matrix, as discussed in Ref. [15].

### 3 Shell model calculation

For the shell model calculation we define the model space to consist of the spherical single-particle orbitals in the  $N = 4$  oscillator shell ( $1d_{5/2}$ ,  $0g_{7/2}$ ,  $1d_{3/2}$ ,  $2s_{1/2}$ ) plus the intruder  $0h_{11/2}$  orbital from the  $N = 5$  oscillator shell. Hereafter this model space is referred to as the *sdg*-shell. This means that our  $P$ -space consists of the proton orbitals outside the  $^{132}\text{Sn}$  core, ranging from the closed  $Z = 50$ ,  $N = 82$  core to the closed  $Z = N = 82$  core.

At present it does not seem possible to calculate the  $P$ -space single-particle energies along the same lines as the effective two-body interaction. The theoretical framework is available, but the results are not accurate enough for our purpose. However, the single-particle energies can be extracted from the experimental  $^{133}\text{Sb}$

spectrum [20], except for the  $2s_{1/2}$  single-particle state which has not yet been measured. For the  $2s_{1/2}$  single-particle energy we have taken the value used by Sagawa *et al.* [10]. The adopted single-particle energies are as displayed in Fig. 1.

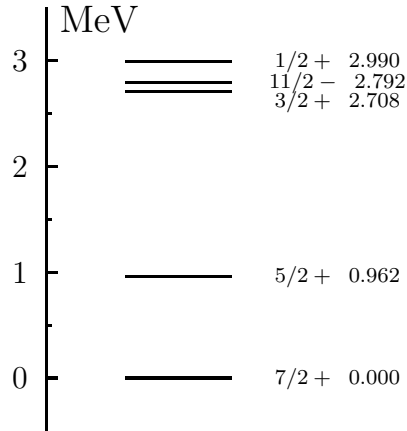


Fig. 1. Adopted single-particle energies for the orbitals  $2s_{1/2}$ ,  $1d_{3/2}$ ,  $1d_{5/2}$ ,  $0g_{7/2}$  and  $h_{11/2}$  in the shell model calculation.

In the shell model calculation, all degrees of freedom within the defined  $P$ -space are included. Thus, the dimension of the problem grows rapidly with increasing number of valence particles as shown in Table 1. Our basic approach to solving the many-body eigenvalue problem is the Lanczos algorithm, a method which was first applied to nuclear physics problems by Whitehead *et al.* [21]. This is an iterative method, where the 10 – 20 low-lying eigenstates of interest are obtained after a rather limited number of iterations. The shell model algorithm used is reviewed in more detail in Ref. [13].

For the low energy region of the Sn isotopes where the main degrees of freedom are valence neutrons filling up the  $sdg$ -shell, a characteristic feature of the even-even nuclei is the remarkably constant spacing between the  $0^+$  ground state and the first excited  $2^+$  state. The  $N = 82$  isotones have a different closed core, but what still should be important is the filling of the  $sdg$ -shell, now with protons. In Fig. 2 we have compared the empirical  $0_1^+ - 2_1^+$  spacing for the Sn isotopes and the  $N = 82$  isotones. As can be seen, the  $N = 82$  isotones do not have the same type of constant  $0_1^+ - 2_1^+$  spacing as is observed for the Sn isotopes. The spacing increases slightly with increasing proton number until the middle of the shell at  $Z = 64$  where there is a sudden increase in the spacing yielding a gap, close to 2 MeV in magnitude.

Small but important differences in the single-particle spectra are found between

Table 1

Number of basis states for the shell model calculation of the  $N = 82$  isotones, with  $1d_{5/2}$ ,  $0g_{7/2}$ ,  $1d_{3/2}$ ,  $2s_{1/2}$  and  $0h_{11/2}$  single particle orbitals.

System	Dimension	System	Dimension	System	Dimension
$^{134}\text{Te}$	36	$^{139}\text{La}$	108 297	$^{144}\text{Sm}$	6 210 638
$^{135}\text{I}$	245	$^{140}\text{Ce}$	323 682	$^{145}\text{Eu}$	9 397 335
$^{136}\text{Xe}$	1 504	$^{141}\text{Pr}$	828 422	$^{146}\text{Gd}$	12 655 280
$^{137}\text{Cs}$	7 451	$^{142}\text{Nd}$	1 853 256	$^{147}\text{Tb}$	15 064 787
$^{138}\text{Ba}$	31 124	$^{143}\text{Pm}$	3 609 550	$^{148}\text{Dy}$	16 010 204

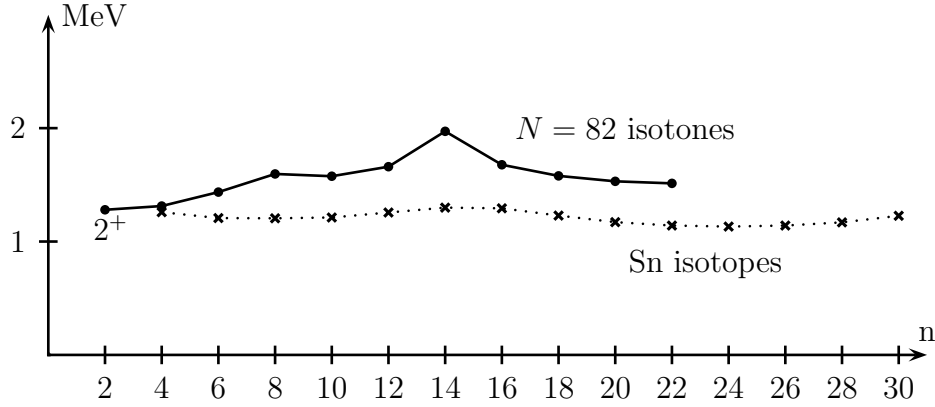


Fig. 2. Experimental excitation energies for the lowest  $2^+$  state in the Sn isotopes compared with the  $N = 82$  isotones, where  $n$  is the number of valence particles relative to  $^{100}\text{Sn}$  and  $^{132}\text{Sn}$  respectively.

the Sn isotopes and the  $N = 82$  isotones. The strong pairing effect which is seen for tin, is due to the nearly degenerate  $1d_{5/2}$  and  $0g_{7/2}$  single-particle orbitals. These orbitals are predicted, from a shell model extrapolation by Grawe *et al.* [22], to be approximately 0.20 MeV apart. From  $^{133}\text{Sb}$  we know that the  $1d_{5/2}$  and  $0g_{7/2}$  orbitals are interchanged relative to  $^{101}\text{Sn}$ , and separated by 0.96 MeV. The larger separation of the two orbitals may explain the less stable  $0_1^+ - 2_1^+$  spacing in the  $N = 82$  isotones.

Much attention has been devoted to  $^{146}\text{Gd}$  and to the question to what extent  $^{146}\text{Gd}$  can be considered as a stable closed subshell nucleus. Similarities between



$^{146}\text{Gd}$  and  $^{208}\text{Pb}$ , like the  $3^-$  first excited state and the large gap between the  $0^+$  ground state and the first excited  $2^+$  state, led to intensive studies [23–25] and speculations about the size of the single-particle energy gap at  $Z = 64$ . However, it now seems clear that  $^{146}\text{Gd}$  has doubly magic properties, but the subshell closure does not appear as pronounced as for  $^{208}\text{Pb}$  [2].

Above we have described some general, qualitative properties of the  $N = 82$  isotones, and it is essential that our microscopic shell model calculation is able to reproduce such phenomena.

#### 4 The $N = 82$ isotones in the framework of the QRPA

The quasiparticle random-phase approximation (QRPA) is here presented as an alternative method to the shell model. The basic ingredients of the QRPA approach used in this work are described in Ref. [26]. We start by solving the BCS equations for both protons and neutrons in a larger space of single-particle orbitals than included in the shell model calculation. Then a QRPA energy matrix is calculated and solved for each spin separately. The nuclear states are obtained as linear combinations of proton-proton and neutron-neutron two-quasiparticle excitations. A bare  $G$ -matrix is used for the interaction and the idea is that quasiparticle excitations replace the effect of the perturbation calculation in the shell model case. Thus, instead of treating core excitations in perturbation theory producing an effective interaction between valence protons, the quasiparticle excitations are explicitly included in the nuclear wave functions. New states may be obtained not present in the shell model approach if a large part of the corresponding wave functions are core excitations. Such configurations are not treated properly in perturbation theory. In the present case the proton single-particle basis is taken to consist of the  $1p0f$  and  $2s1d0g$  oscillator major shells complemented with the  $0h_{11/2}$  intruder state from the major shell above. This leaves  $Z = 20$  as an inert proton core. For neutrons we have chosen the valence space to consist of the  $2s1d0g_{7/2}$  and  $2p1f0h$  major shells leaving  $N = 50$  as the neutron core.

In the QRPA calculation, the two-body interaction used to construct the energy matrix, is obtained from the Bonn one-boson-exchange potential giving the same nuclear  $G$ -matrix discussed in Sect. 2. In this calculation the bare  $G$ -matrix has been applied and no attempts are made to create a model-space adapted effective interaction because the single-particle space for the QRPA is relatively large. In order to have as equal as possible starting points in the QRPA and the shell model approaches, we use the proton single-particle energies as shown in Fig. 1. For protons in the  $1p0f0g_{9/2}$  shell and neutrons in the  $2s1d0g_{7/2}0h_{11/2}$  and

$1p0f0g_{9/2}$  shells we employ Woods-Saxon single-particle energies calculated using the parametrization of Bohr and Mottelson [27].

The QRPA calculation is slightly different from the more traditional ones as discussed in Ref. [26]. It has been pointed out in Ref. [8] that pairing effects are strong in the  $N = 82$  isotones and this means that it is essential to exploit the available experimental data on pairing gaps and single-quasiparticle energies if one wants to obtain an improved QRPA description of the low-energy properties of the nuclei under study. Typically, certain matrix elements of the  $G$ -matrix may be scaled in order to reproduce the systematics of pairing in certain isotopes and isotones, as done in Refs. [26,28,29]. However, in this work we have not performed such a refitting of the nuclear  $G$ -matrix. If one adjusts the  $G$ -matrix by some scaling constants in order to have a better reproduction of the spectra in the QRPA one introduces many-body effects whose origin are difficult to retrace. Although the QRPA may not give the best results for the spectroscopy, we feel that an equal starting point, same  $G$ -matrix and single-particle energies, may offer a better possibility for studying differences between the QRPA and the shell model.

From the present discussion and the one in Sect. 2 it is obvious that the QRPA approach exhibits two important differences compared to the shell model approach. First, the single-particle basis for protons is larger for the QRPA allowing for proton core excitations across the  $Z = 50$  shell gap. Second, also the neutrons are active yielding neutron core excitations across the  $N = 82$  shell gap. This might become important for the description of some low-energy collective excitations of the even  $N = 82$  isotones. In the shell model approach these degrees of freedom are supposed to be accounted for by terms included in the perturbative expansion of the effective interaction. Substantial differences in the two approaches may therefore reveal whether such low-energy collective excitations are accounted for in the shell model approach where the calculations are done within a smaller single-particle space, but with a complete set of many-body basis states within the chosen model space.

## 5 Numerical results and discussion

### 5.1 Energy levels

The calculated energy eigenstates of the QRPA and the shell model (SM) along with the experimental energy levels are presented in Tables 2, 3 and 4. If nothing else is specified data are taken from the data base of the National Nuclear Data

Center, Brookhaven National Laboratory, Upton, N.Y., USA. A large number of E2 transitions are experimentally known for the  $N = 82$  isotones. Data for some selected transitions are presented in Table 5 and compared with our theoretical predictions. Some E3 transitions are also presented in the same table.

In the SM calculation of E2 transitions an effective proton charge  $e_p^{\text{eff}}(\text{SM}) = 1.4e$  is used in agreement with the discussion in [27]. Our model space which includes the  $2s1d0g_{7/2}0h_{11/2}$  single-particle orbitals would require an effective E2 operator which may be calculated along the same lines as the effective interaction discussed in Sect. 2. However, at present we limit ourselves to a constant effective E2 charge. For the QRPA a larger single-particle space is explicitly included in the calculation and an effective E2 charge  $e_p^{\text{eff}}(\text{QRPA}) = 1.0e$  is appropriate.

There are two important questions related to the present calculation. First, can a medium dependent effective interaction which is calculated starting from the free nucleon-nucleon (NN) potential be used in medium-heavy nuclei? Secondly, which states in the  $N = 82$  isotones are well described by the chosen model space? As discussed in Sect. 2, our approximations lie in the choice of model space and selection of many-body diagrams in the definition of the effective interaction. The only parameters which enter our theory are those which define the NN potential. Thus, in case of disagreements with observation it is important not to modify the derived effective interaction in order to get an improved reproduction of the data. Such disagreements may point to degrees of freedom not accounted for in our many-body scheme.

In view of these restrictions our results are rather good. For both models the deviation of our calculated energy levels from the experimental ones is generally within 0.1 – 0.3 MeV. Up to five  $2^+$  states, three  $4^+$  states and two  $6^+$  states are well reproduced throughout the sequence of isotones indicating that the degrees of freedom represented by the chosen proton model space are the relevant ones. A decomposition of the QRPA  $2_1^+$  wave functions shows that these states are constructed mainly of two-quasiparticle proton excitations within the  $sdg$ -shell, a picture which is consistent with the SM. There is a very small contribution of neutron core excitations in the wave functions, a contribution which increases slightly towards the middle of the shell. Furthermore, the high-spin states  $8^+$  and  $10^+$  are well reproduced except for  $^{144}\text{Sm}$  where the theoretical states are too high in energy (0.58 MeV for  $8^+$  and 0.97 MeV for  $10^+$ ). This may indicate that other degrees of freedom are important for these high spin states.

With one exception the known E2 transitions are well reproduced. A typical feature of the even  $N = 82$  isotones is enhanced E2 transitions between the first excited  $2^+$  state and the  $0^+$  ground state with strengths around 10 W.u. These transitions strengths are well reproduced by the proton degrees of freedom

within the SM valence space with some additional polarization charge which can be described in perturbation theory. This effect is also seen in the structure of the  $2_1^+$  state in the QRPA framework, where a large number of two-quasiparticle components are present and contribute coherently to the E2 transition rate. We obtain  $4_1^+ \rightarrow 2_1^+$  and  $2_1^+ \rightarrow 0_1^+$  E2 transitions in good agreement with experiment. The  $6_1^+ \rightarrow 4_1^+$  transition in  $^{134}\text{Te}$  is also reasonably well reproduced. For the other isotones this transition is weak, and we have more difficulties in reproducing these data. In spite of the rather large deviation in energy between the calculated  $8_1^+$  and  $10_1^+$  states and the corresponding experimental states, the E2  $10_1^+ \rightarrow 8_1^+$  values are in good agreement with data.

An SM calculation for  $^{146}\text{Gd}$  is difficult due to the large number of basis states, see Table 1. At present we have only calculated the ground state and the first excited  $2^+$  state. The  $0_1^+ - 2_1^+$  spacing is found to be 1.864 MeV and compares well to the experimental value of 1.972 MeV. However, the experimental increase in energy for the  $2^+$  state from  $^{144}\text{Sm}$  to  $^{146}\text{Gd}$  indicates shell closure of the  $d_{5/2}g_{7/2}$  single-particle orbits. The SM calculation reproduces this feature but not as sharp as found experimentally. The  $0_1^+ - 2_1^+$  spacing throughout the sequence of isotones is shown in Fig. 3. The SM reproduces the weak increase reasonably well but with some small deviations at the endpoints. The QRPA predicts a constant spacing due to the use of the BCS approximation.

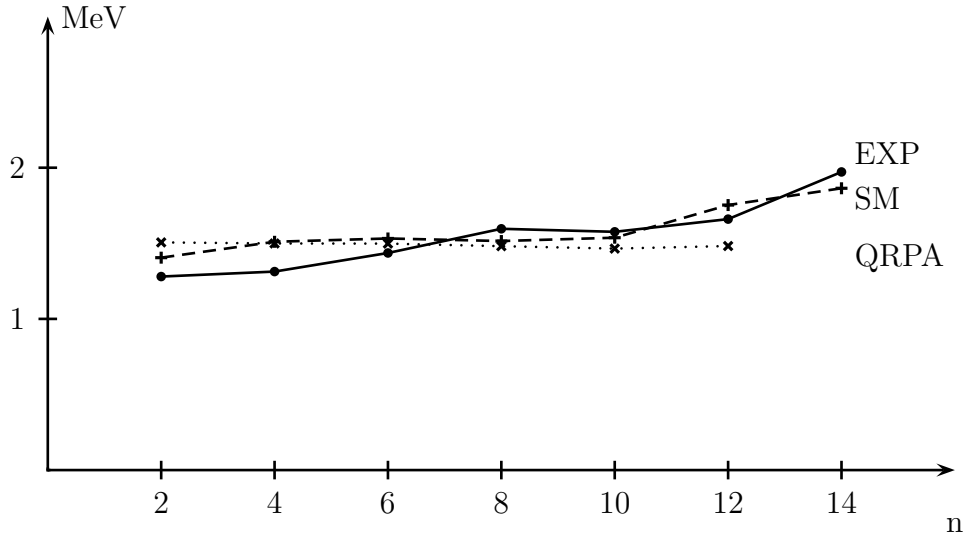


Fig. 3. The  $2_1^+$  state in the  $N = 82$  isotones, where  $n$  is the number of valence particles relative to  $^{132}\text{Sn}$ .

In addition to the  $0^+$  ground state several excited states with  $J = 0^+$  are known experimentally. The SM reproduces these states reasonably well. However, one  $0_2^+ \rightarrow 2_1^+$  E2 transition in  $^{140}\text{C}$  has been measured to 11.5 Wu and our SM calculation fails in reproducing the strength of this transition by a factor of more than

Table 2

Low-lying states for  $^{134}\text{Te}$  and  $^{136}\text{Xe}$ . Experimental angular momentum values in parentheses are tentative. Energies are given in MeV.

$^{134}\text{Te}$					$^{136}\text{Xe}$				
$J^\pi$	QRPA	SM	Exp		$J^\pi$	QRPA	SM	Exp	
$0_2^+$	1.936	2.715			$0_2^+$	1.414	2.174	2.582	$0^+$
$0_3^+$	2.686	6.316			$0_3^+$	2.387	3.049		$0^+$
$0_4^+$	3.876	7.141			$0_4^+$	4.124	3.762	4.320	
$2_1^+$	1.506	1.405	1.279	$2^+$	$2_1^+$	1.499	1.510	1.313	$2^+$
$2_2^+$	2.619	2.646	2.464	$(2^+)$	$2_2^+$	2.415	2.382	2.290	$2^+$
$2_3^+$	2.928	3.258	2.934	$(2^+)$	$2_3^+$	2.465	2.674	2.415	$2^+$
$2_4^+$	2.992	4.063			$2_4^+$	2.720	2.706	2.634	$2^+$
$2_5^+$	3.493	5.196			$2_5^+$	3.300	2.944	2.849	$2^{(+)}$
$3_1^+$	2.006	2.793			$3_1^+$	2.137	2.505	2.126	$3^+, 4^+$
$3_1^-$	3.374				$3_1^-$	3.095		3.275	$3^-$
$3_2^-$	4.425	4.313			$3_2^-$	4.181	3.992		
$4_1^+$	1.849	1.717	1.570	$4^+$	$4_1^+$	1.956	1.895	1.694	$4^+$
$4_2^+$	2.588	2.701			$4_2^+$	2.463	2.400	2.465	$(4^+)$
$4_3^+$	3.190	3.548			$4_3^+$	2.744	2.575	2.560	$4^+$
$5_1^+$	2.006	2.826	2.727	$(5^+)$	$5_1^+$	2.137	2.448	2.444	5
$6_1^+$	1.996	1.893	1.691	$6^+$	$6_1^+$	2.110	2.095	1.892	$6^+$
$6_2^+$	2.348	2.394	2.396	$(6^+)$	$6_2^+$	2.266	2.166	2.262	$6^+$
$8_1^+$	3.424	7.362	4.557	$8^+$	$8_1^+$	2.914	3.327		
$10_1^+$	3.524	7.538	5.622	$10^+$	$10_1^+$	3.014	3.671		

four. It is known that in shell model calculations with realistic interactions E2 transitions like  $2_1^+ \rightarrow 0_1^+$  will be large whereas  $0_n^+ \rightarrow 2_1^+$  E2 transitions are small. This feature is due to an enhanced quadrupole character of the effective interaction. Phenomenon like the present one with a large  $0_2^+ \rightarrow 2_1^+$  transition indicates the importance of other degrees of freedom in the wave functions, probably a significant core excitation. For all the isotones more experimental information is therefore urgently needed in order to identify the properties of these states in more detail.

Table 3

Low-lying states for  $^{138}\text{Ba}$  and  $^{140}\text{Ce}$ . Experimental angular momentum values in parentheses are tentative. Energies are given in MeV.

$^{138}\text{Ba}$					$^{140}\text{Ce}$				
$J^\pi$	QRPA	SM	Exp		$J^\pi$	QRPA	SM	Exp	
$0_2^+$	1.246	2.105	2.340	$0^+$	$0_2^+$	2.209	2.234	1.903	$0^+$
$0_3^+$	2.210	2.978	3.612	$(0^+)$	$0_3^+$	2.246	3.054	3.017	$0^+$
$0_4^+$	4.126	3.838	3.484		$0_4^+$	4.146	3.589	3.226	$0^+$
$2_1^+$	1.498	1.532	1.436	$2^+$	$2_1^+$	1.481	1.515	1.596	$2^+$
$2_2^+$	2.257	2.381	2.190	$(1, 2, 3)$	$2_2^+$	2.412	2.447	2.348	$2^+$
$2_3^+$	2.383	2.564	2.218	$2^+$	$2_3^+$	2.617	2.630	2.521	$2^+$
$2_4^+$	2.587	2.862	2.583	$(1^+, 2^+)$	$2_4^+$	3.086	4.724	2.900	$2^+$
$2_5^+$	3.164	3.003	2.640	$2^+$	$2_5^+$	3.255	6.042	3.001	$2^+$
$3_1^+$	2.347	2.479	2.446	$3^+$	$3_1^+$	2.510	2.557	2.412	$3^+$
$3_1^-$	2.737		2.881	$3^-$	$3_1^-$	2.320		2.464	$3^-$
$3_2^-$	3.919	3.699	3.647	$(3)^-$	$3_2^-$	3.704		3.040	$3^-$
$3_3^-$	4.789	4.118	3.923	$(3)^-$	$3_3^-$	4.865	3.484	3.473	$3^-$
$4_1^+$	2.080	2.035	1.898	$4^+$	$4_1^+$	2.137	2.134	2.083	$4^+$
$4_2^+$	2.442	2.422	2.308	$4^+$	$4_2^+$	2.506	2.506	2.481	$4^+$
$4_3^+$	2.589	2.512	2.583	$4^+$	$4_3^+$	2.608	2.542	2.516	$3^+, 4^+$
$4_4^+$	3.606	2.814	2.779	$4^+$	$4_4^+$	3.292	4.701	3.331	$4^+$
$5_1^+$	2.347	2.421	2.415	$5^+$	$5_1^+$	2.510	2.516	2.350	$5^+$
$6_1^+$	2.155	2.178	2.091	$6^+$	$6_1^+$	2.211	2.238	2.108	$6^+$
$6_2^+$	2.386	2.425	2.203	$6^+$	$6_2^+$	2.667	2.588	2.629	$6^+$
$8_1^+$	2.759	3.424	3.184	$8^+$	$8_1^+$	3.761	3.476	3.513	$8^+$
$10_1^+$	2.859	3.904	3.622	$10^+$	$10_1^+$	3.861	4.065	3.715	$10^+$

In the QRPA the first eigenstate emerging from the diagonalization of the two-body interaction in the  $0^+$  coupled two-quasiparticle basis, is a spurious one [30] and related to the ground state. A convenient feature of the QRPA approach is that all the other eigenstates are free from such a spuriousity. The energy of the spurious state becomes zero leaving the rest of the excited  $0^+$  states as physical

Table 4

Low-lying states for  $^{142}\text{Nd}$  and  $^{144}\text{Sm}$ . Experimental angular momentum values in parentheses are tentative. Energies are given in MeV.

$^{142}\text{Nd}$					$^{144}\text{Sm}$				
$J^\pi$	QRPA	SM	Exp		$J^\pi$	QRPA	SM	Exp	
$0_2^+$	2.402	2.377	2.217	$0^+$	$0_2^+$	1.947	2.397	2.478	$0^+$
$0_3^+$	3.074	2.674	2.978	$0^+$	$0_3^+$	2.675		2.827	$0^+$
$0_4^+$	3.457	3.653	3.583	$(0^+)$	$0_4^+$	2.896		3.142	$0^+$
$2_1^+$	1.465	1.537	1.576	$2^+$	$2_1^+$	1.482	1.753	1.660	$2^+$
$2_2^+$	2.516	2.510	2.385	$2^+$	$2_2^+$	2.577	2.536	2.423	$2^+$
$2_3^+$	2.841	2.676	2.846	$2^+$	$2_3^+$	2.610	2.639	2.661	$(2^+)^a)$
$2_4^+$	3.070		3.046	$(2^+)$	$2_4^+$	3.123	2.793	2.799	$2^+$
$2_5^+$	3.375		3.128	$(1, 2^+)$	$2_5^+$	3.249		3.318	$2^+$
$3_1^+$	2.428	2.644	2.548	$3^+$	$3_1^+$	2.528		2.687	$3^{(+)^a)$
$3_1^-$	1.882		2.085	$3^-$	$3_1^-$	1.477		1.810	$3^-$
$3_2^-$	3.547	3.325	3.366	$(3)^-$	$3_2^-$	3.446	3.196	3.228	$3^-$
$4_1^+$	2.140	2.235	2.101	$4^+$	$4_1^+$	2.196	2.390	2.191	$4^+$
$4_2^+$	2.593	2.642	2.438	$4^+$	$4_2^+$	2.771	2.737	2.588	$4^+$
$4_3^+$	2.932	2.667	2.738	4	$4_3^+$	2.787	2.830	2.884	$4^+$
$5_1^+$	2.428	2.626	2.514	$5^+$	$5_1^+$	2.528		2.704	$(5^+)^a)$
$6_1^+$	2.364	2.316	2.210	$6^+$	$6_1^+$	2.656	2.363	2.323	$6^+$
$6_2^+$	3.062		2.887	$6^+$	$6_2^+$	2.875		2.729	$(6^+)$
$8_1^+$	4.349	3.819	3.454	$8^+$	$8_1^+$	3.636	4.193	3.651	8
$10_1^+$	4.451	4.080	3.926	$10^+$	$10_1^+$	3.735	5.195	4.221	10

<sup>a)</sup> Ref. [7]

ones. As seen from tables 2 and 3 the  $0^+$  QRPA reproduces the excited  $0^+$  states reasonably well in the middle of the shell whereas it fails at the beginning and at the end, again due to the basic BCS approximation used.

Of the negative parity states we have only calculated the  $3^-$  states. Such states may be generated through the  $h_{11/2}$  negative parity orbit or through strong oc-

Table 5

E2 and E3 transitions for  $^{134}\text{Te}$  -  $^{144}\text{Sm}$ . For theory  $e_p^{\text{eff}}(\text{SM}) = 1.4e$  and  $e_p^{\text{eff}}(\text{QRPA}) = 1.0e$  for E2 transitions, while  $e_p^{\text{eff}}(\text{SM}) = 1.0e$  and  $e_p^{\text{eff}}(\text{QRPA}) = 1.0e$  for E3 transitions. All entries are given in Weisskopf units.

Transition		Calc	Exp	Calc	Exp	Calc	Exp
		A = 134		A = 136		A = 138	
B(E2; $2_1^+ \rightarrow 0_1^+$ )	SM	3.5	> 0.024	7.0	9 (4)	10.9	11.4 (3)
	QRPA	4.6		8.4		11.5	
B(E2; $4_1^+ \rightarrow 2_1^+$ )	SM	3.7	3.9 (4)	1.5	1.25 (6)	1.5	0.286 (11)
B(E2; $6_1^+ \rightarrow 4_1^+$ )	SM	1.7	2.04 (5)	0.3	0.0132 (5)	< $10^{-4}$	0.053 (7)
B(E2; $10_1^+ \rightarrow 8_1^+$ )	SM					1.1	1.59 (22)
B(E3; $3_1^- \rightarrow 0_1^+$ )	SM	$1.6 \cdot 10^{-2}$		0.2		1.6	0.133 (13)
	QRPA	12.6		12.3		12.7	
		A = 140		A = 142		A = 144	
B(E2; $2_1^+ \rightarrow 0_1^+$ )	SM	13.4	16.6 (24)	14.1	12.04 (18)	15.1	11.5 (3) <sup>a)</sup>
	QRPA	14.8		14.2		11.2	
B(E2; $4_1^+ \rightarrow 2_1^+$ )	SM	0.1	0.137 (1)				
B(E2; $6_1^+ \rightarrow 4_1^+$ )	SM	0.2	0.28 (6)	0.05	0.0179 (12)	0.01	0.188 (10)
B(E2; $10_1^+ \rightarrow 8_1^+$ )	SM	0.5	0.46 (13)				
B(E2; $0_2^+ \rightarrow 2_1^+$ )	SM	2.6	11.5 (9)				
B(E3; $3_1^- \rightarrow 0_1^+$ )	SM	2.9	> 5.6(2)	3.9	28.6		38 (3) <sup>b)</sup>
	QRPA	13.9		16.2		19.5	

<sup>a)</sup> Ref. [6]

<sup>b)</sup> Ref. [4]

tupole core excitations. The SM should reproduce states of the first type but fail for states of the second. On the other hand we expect QRPA to describe strong octupole vibrational states since the single-particle orbits of the core are explicitly included. Contrary to the  $2^+$ ,  $4^+$  and  $6^+$  states we find for the  $3^-$  states clear differences between the two models. The QRPA produces always a low-lying  $3^-$  state not found in the SM calculation. This may be a good candidate for a col-



lective octupole state. Unfortunately, we can not draw clear conclusions from the present experimental data. In particular, the experimental information on the  $E3(3^- \rightarrow 0^+)$  transitions as seen in Table 5 is sparse and somewhat confusing. In  $^{142}\text{Nd}$  and  $^{144}\text{Sm}$  a strong  $E3(3^- \rightarrow 0^+)$  is found experimentally in agreement with the QRPA prediction. On the other hand a very weak  $E3(3^- \rightarrow 0^+)$  transition is measured in  $^{136}\text{Xe}$  and is more in line with the SM results. In the other cases of interest no experimental data are known. Thus as a temporary conclusion we have in Tables 2, 3 and 4 for the SM results excluded the lowest lying experimental  $3^-$  when we identify our calculation with experiment. The QRPA seems to reproduce all  $3^-$  states with a question mark for the  $3^-$  state in  $^{136}\text{Xe}$ .

Guided by our calculations we suggest the following interpretation for states given with several alternative experimental spin assignments:

The state in  $^{136}\text{Xe}$  at 2.126 MeV is given the two alternative angular momentum values  $J^\pi = 3^+, 4^+$ . Our calculations give no  $4^+$  state corresponding to this state, but the QRPA calculations predict a  $3^+$  state with almost this energy.

In  $^{138}\text{Ba}$  there are two states where the angular momentum assignment is tentative, and different values are considered. The first one is at 2.190 MeV of excitation energy with  $J = (1, 2, 3)$ , and the other one is at 2.583 MeV of excitation with  $J^\pi = (1^+, 2^+)$ . Our calculations suggest that both states have  $J^\pi = 2^+$ .

In  $^{140}\text{Ce}$  there are two alternative assignments for the state of 2.516 MeV excitation energy,  $J^\pi = 3^+$  and  $4^+$ . Both our models predict a  $4^+$  state near this energy. Our calculations do also give a  $3^+$  state in the same energy region, but this most probably corresponds to the experimental  $3_1^+$  state at 2.464 MeV.

Of the negative parity states we have only calculated the  $3^-$  states. Here the deviation between experiment and the SM is significant, whereas the QRPA reproduces the data reasonably well, except for  $^{144}\text{Sm}$ .

The shell model is not able to reproduce the first  $3^-$  state for any of the isotones, while both QRPA approaches yield the lowest-lying  $3^-$  states in nice agreement with experiment. The QRPA wave functions indicate that these states are strongly collective, and that they are a mixture of both proton and neutron degrees of freedom. The philosophy of the effective theory is that the main components of the shell model wave functions have the origin within the model space ( $P$ -space components), and the rest ( $Q$ -space components) are included through the perturbation technique. Not all degrees of freedom are taken into account this way, like for instance neutron core excitations. The above mentioned  $3^-$  state, if assuming a strong mixture of neutron degrees of freedom, can therefore not be described within the frame of the shell model calculation. However, the  $3^-$  states, which according to the QRPA are of two-quasiparticle character and con-

sist of pure proton excitations, are very well described by the shell model. This also indicates that there is a minimal mixing between the different  $3^-$  states. Our interpretation is then that the second experimental  $3^-$  states contain mainly two-quasiproton excitations with one exception. In  $^{140}\text{Ce}$ , it is the third experimental  $3^-$  state which most probably corresponds to the two-quasiproton  $3^-$  state. The  $3^-$  state which appears in  $^{140}\text{Ce}$  at an excitation energy of 3.040 MeV can neither be described within the QRPA nor the shell model. Similar low-lying  $3^-$  states, which can not be described within either of our models, are also observed in the other  $N = 82$  isotones. A possible explanation of the nature of these  $3^-$  states might be that they are octupole deformed and possibly created by neutron two-particle-two-hole excitations. These excitations activate the long-range part of the proton-neutron interaction and yield to deformation.

Calculations of the E3 transition  $3^- \rightarrow 0^+$  can give information on whether our models succeed in describing the structure of the  $3^-$  states or not. No  $B(\text{E}3; 3_1^- \rightarrow 0_1^+)$  data are available for  $^{134}\text{Te}$  and  $^{136}\text{Xe}$ . In  $^{138}\text{Ba}$  there is a E3 transition rate from the  $3_1^-$  to the ground state which is measured to be 0.133 (13) W.u. There are uncertainties concerning the lifetime of the  $3_1^-$  state in  $^{140}\text{Ce}$ . An experiment by Grinberg et al. [31] has given an upper limit for the lifetime  $< 0.1$  ns, which corresponds to  $B(\text{E}3; 3_1^- \rightarrow 0_1^+) > 5.6(2)$  W.u. In  $^{142}\text{Nd}$  and  $^{144}\text{Sm}$  the  $B(\text{E}3; 3_1^- \rightarrow 0_1^+)$  are reported to be 28.6 W.u. and 38 (3) W.u., respectively.

The QRPA E3 transitions rates are fairly constant and vary from 12.6 W.u. in  $^{134}\text{Te}$  to 19.6 W.u. in  $^{144}\text{Sm}$ . The size of the calculated  $B(\text{E}3)$  values is a sign of collectivity and supports the picture we already have that the QRPA  $3_1^-$  states are due to excitations of the core. For the same reasons as in the E2 calculations, no effective charge is here used.

The SM  $B(\text{E}3)$  values increase with increasing number of valence particles. An effective charge of  $e_{\text{eff}} = 2.7e$  will be required in order to reproduce the  $B(\text{E}3; 3_1^- \rightarrow 0_1^+)$  in  $^{142}\text{Nd}$ . Due to the strong dependence of the number of active particles it is likely to believe that the  $3_1^-$  SM states are results of pure excitations of the valence protons.

Before we can draw further conclusions more thorough measurements of the  $3^-$  lifetime in  $^{140}\text{Ce}$  is needed, and we will also encourage the experimentalists to seek more information about the  $3^-$  states in the  $N=82$  isotones lighter than  $^{140}\text{Ce}$ .

## 5.2 Generalized seniority

The proton occupation number for each  $(lj)$  value is determined within the shell model and compared with experiment and the BCS occupations underlying the

QRPA calculation in Table 6. For both the shell model and the BCS the calculated ground states have too large components of  $d_{5/2}$ , but the sum of the  $g_{7/2}$  and  $d_{5/2}$  occupation numbers are close to the experimental values. The proton occupation numbers, calculated for the ground state of  $^{146}\text{Gd}$ , show that on the average 12 out of 14 valence particles are occupying the  $0g_{7/2}$  and  $1d_{5/2}$  orbitals. As a general observation one can see from Table 6 that there is, in general, a close correspondence between the shell model occupations and the BCS occupations.

The results from Table 6 indicate that pairing effects are likely to be important. In order to test whether generalized seniority is conserved, we construct the pair correlation operator for creating a generalized seniority  $v = 0$  pair

$$S^\dagger = \sum_j \frac{1}{\sqrt{2j+1}} C_j \sum_{m \geq 0} (-1)^{j-m} a_{jm}^\dagger a_{j-m}^\dagger, \quad (9)$$

where the coefficients  $C_j$  are obtained from the ground state of  $^{134}\text{Te}$ . Similarly the generalized seniority  $v = 2$  operator takes the form

$$D_{J=2, M=0}^\dagger = \sum_{j \leq j', m \geq 0} (1 + \delta_{j,j'})^{-1/2} \beta_{j,j'} \langle j m j' - m | 2 0 \rangle a_{jm}^\dagger a_{j'-m}^\dagger, \quad (10)$$

where the coefficients  $\beta_{j,j'}$  are obtained from the first excited  $2^+$  state of  $^{134}\text{Te}$ .

With our shell model wave functions we evaluate the squared overlaps  $|\langle A; J^\pi | S^\dagger | A-2; J^\pi \rangle|^2$  and  $|\langle A; 2_1^+ | D_{J=2, M=0}^\dagger | A-2; 0_1^+ \rangle|^2$ . The results are given in Tables 7 and 8.

The ground state can be well described within a generalized seniority scheme. More than 95% of the wave function for the  $(A)$  system is given as the  $(A-2)$  system plus a seniority-zero pair. Also for the  $2_1^+$ ,  $4_1^+$  and  $6_1^+$  states, generalized seniority is an approximately conserved quantum number. The overlap is in general 85 – 95%.

Andreozzi *et al.* [8] pointed out the importance of seniority-zero components in the structure of the  $0_2^+$  states. They managed to reproduce nicely the  $0_2^+$  energy levels within their pairing model, but no E2 transitions were calculated which would give a more sensitive test of the wave functions.

In  $^{134}\text{Te}$  the  $0_2^+$  state is not yet observed, but for the other nuclei,  $^{136}\text{Xe}$  -  $^{144}\text{Sm}$ , data is now available. As mentioned before we are not able to give such a good description of these states. Only 75 – 85% of our states are given as the  $0_2^+$  state in the  $(A-2)$  system plus a seniority-zero pair.

Table 6

Experimental (Ref. [32]) and calculated proton occupation numbers for the ground states of the even-mass  $N = 82$  isotones.

s.p. orbitals	$g_{7/2}$	$d_{5/2}$	$h_{11/2}$	$d_{3/2}$	$s_{1/2}$	$g_{7/2} + d_{5/2}$
$^{134}\text{Te}$						
SM	1.56	0.25	0.13	0.05	0.02	1.81
BCS	1.60	0.30	0.20	0.04	0.02	1.90
$^{136}\text{Xe}$						
Exp	3.5(4)	0.5(2)	0.0(7)	0.0(2)	0.0(2)	4.0(6)
SM	2.79	0.76	0.28	0.12	0.04	3.55
BCS	3.02	0.63	0.46	0.09	0.03	3.65
$^{138}\text{Ba}$						
Exp	4.3(4)	0.7(3)	1.0(8)	0.0(2)	0.0(2)	5.0(7)
SM	3.69	1.57	0.45	0.22	0.07	5.26
BCS	4.20	1.27	0.59	0.15	0.05	5.47
$^{140}\text{Ce}$						
Exp	5.6(3)	1.8(2)	0.6(4)	0.0(2)	0.0(2)	7.4(5)
SM	4.44	2.50	0.62	0.34	0.16	6.94
BCS	4.55	2.55	0.80	0.32	0.09	7.10
$^{142}\text{Nd}$						
Exp	5.7(3)	2.6(3)	1.3(5)	0.2(1)	0.2(1)	8.3(6)
SM	5.17	3.43	0.78	0.46	0.16	8.60
BCS	5.62	3.32	0.86	0.36	0.10	8.94
$^{144}\text{Sm}$						
Exp	6.3(2)	3.6(2)	1.6(3)	0.3(1)	0.2(1)	9.9(4)
SM	5.90	4.30	0.96	0.61	0.23	10.20
BCS	6.63	4.29	0.82	0.32	0.12	10.92
$^{146}\text{Gd}$						
SM	6.72	4.96	1.15	0.82	0.35	11.68
BCS	7.28	5.14	0.98	0.43	0.30	12.42

Table 7

Generalized seniority overlap  $|\langle A; J_f | S^\dagger | A - 2; J_i \rangle|^2$  where  $J_i = J_f$  and the generalized seniority overlap  $|\langle A; J_f | D^\dagger | A - 2; J_i \rangle|^2$  with  $J_i = 0$  and  $J_f = 2$  for the low-lying eigenstates of  $^{134}\text{Te} - ^{140}\text{Ce}$ .

$A - 2 \rightarrow A$	$^{134}\text{Te} \rightarrow ^{136}\text{Xe}$	$^{136}\text{Xe} \rightarrow ^{138}\text{Ba}$	$^{138}\text{Ba} \rightarrow ^{140}\text{Ce}$
$J_i^\pi \rightarrow J_f^\pi$	$A = 136$	138	140
$0_1^+(v=0) \rightarrow 0_1^+(v=0)$	0.982	0.962	0.957
$2_1^+(v=2) \rightarrow 2_1^+(v=2)$	0.939	0.899	0.931
$4_1^+(v=2) \rightarrow 4_1^+(v=2)$	0.948	0.967	0.928
$6_1^+(v=2) \rightarrow 6_1^+(v=2)$	0.896	0.753	0.913
$0_2^+(v=0) \rightarrow 0_2^+(v=0)$	0.853	0.871	0.761
$0_1^+(v=0) \rightarrow 2_1^+(v=2)$	0.939	0.761	0.613

Table 8

Generalized seniority overlap  $|\langle A; J_f | S^\dagger | A - 2; J_i \rangle|^2$  where  $J_i = J_f$  and the generalized seniority overlap  $|\langle A; J_f | D^\dagger | A - 2; J_i \rangle|^2$  with  $J_i = 0$  and  $J_f = 2$  for the low-lying eigenstates of  $^{140}\text{Ce} - ^{144}\text{Sm}$ .

$A - 2 \rightarrow A$	$^{140}\text{Ce} \rightarrow ^{142}\text{Nd}$	$^{142}\text{Nd} \rightarrow ^{144}\text{Sm}$
$J_i^\pi \rightarrow J_f^\pi$	$A = 142$	144
$0_1^+(v=0) \rightarrow 0_1^+(v=0)$	0.958	0.959
$2_1^+(v=2) \rightarrow 2_1^+(v=2)$	0.911	0.889
$4_1^+(v=2) \rightarrow 4_1^+(v=2)$	0.888	0.824
$6_1^+(v=2) \rightarrow 6_1^+(v=2)$	0.915	0.866
$0_2^+(v=0) \rightarrow 0_2^+(v=0)$	0.796	0.781
$0_1^+(v=0) \rightarrow 2_1^+(v=2)$	0.513	0.475

## 6 Conclusions

In this work a comprehensive study of the  $N = 82$  isotones has been presented. We have performed a large-basis shell model calculation with 2 – 12 valence protons outside the doubly magic nucleus  $^{132}\text{Sn}$ . The main ingredient in the shell model calculation is a realistic, microscopic two-body effective interaction derived from a modern meson-exchange NN potential using many-body perturbation theory.

The philosophy behind the perturbative approach is to include degrees of freedom not accounted for in the model space defining the effective interaction and the shell-model problem. The hope is then that degrees of freedom not included in the shell-model space can be accounted for by such renormalized effective interactions. Differences which may arise between the shell-model approach and the QRPA, where a larger single-particle basis is employed, may then shed light on the strengths and the limitations of the two approaches. As seen from our results, the low-lying states of the even  $N = 82$  isotones are, in general, very well described, both by the shell model and the QRPA. The fact that the QRPA allows for proton and neutron core excitations, gives this model the flexibility to describe some collective excitations which are out of reach of the present shell model description. An example are the first excited  $3^-$  states, which can not be described by the shell model. The QRPA indicates that all these  $3_1^-$  states are strongly collective, and that also non-negligible components of neutron excitations contribute. However, the somewhat higher-lying  $3^-$  states, implied by the QRPA to be of two-quasiproton character, are nicely described by the shell model. There are however other  $3^-$  states that can not be described by any of the models, i.e. in  $^{140}\text{Ce}$ .

The enhanced E2 transitions between the first excited  $2^+$  state and the  $0^+$  ground state, indicate that the  $2_1^+$  states are of vibrational collective nature. With both models we obtain  $B(E2; 2_1^+ \rightarrow 0_1^+)$  values in good agreement with experiment. This is an indication that the calculated wave functions for these states contain the relevant components. In general, the shell model does also give E2 transitions between the other yrast states in good agreement with data.

The aim of this work was to test a new effective interaction for protons outside the closed  $^{132}\text{Sn}$  core. In view of the fact that this is a truly microscopic calculation, with very few parameters, the agreement with data is remarkably good. Our effective interaction seems to be more successful in the region of medium heavy nuclei than for light nuclei (oxygen and calcium regions). The individual degrees of freedom may be more important for light nuclei than for heavier systems, and therefore the results more sensitive to the fine details of the effective interaction.

This work has been supported by the NorFA (Nordic Academy for Advanced Study). The work of M.H.J. has been supported by the Instituto Trentino di Cultura, Italy, and the Research Council of Norway (NFR). The calculations have been carried out in the IBM cluster at the University of Oslo. Support for this from the NFR is acknowledged.

## References

- [1] A. Abbas, Phys. Rev. C 29 (1984) 1033.
- [2] N.R. Walet, P. Stoop and P.W.M. Glaudemans, Z. Phys. A 332 (1989) 9.
- [3] S.W. Yates, R. Julin, P. Kleinheinz, B. Rubio, L.G. Mann, A. Henry, W. Stöfl, D.J. Decman and J. Blomqvist, Z. Phys. A 324 (1986) 417.
- [4] A.F. Barfield, P. von Brentano, A. Dewald, N.V. Zamfir, D. Bucurescu, M. Ivascu and O. Scholten, Z. Phys. A 332 (1989) 29.
- [5] H.H. Pitz, R.D. Heil, U. Kneissl, S. Lindenstruth, U. Seemann and R. Stock, Nucl. Phys. A 509 (1990) 587.
- [6] R.A. Gatenby, J.R. Vanhoy, E.M. Baum, E.L. Johnson, S.W. Yates, T. Belgya, B. Fazekas, A. Veres and G. Molnar, Phys. Rev. C 41 (1990) R414.
- [7] R.A. Gatenby, E.L. Johnson, E.M. Baum, S.W. Yates, D. Wang, J.R. Vanhoy, M.T. McEllistream, T. Belgya, B. Fazekas and G. Molnar, Nucl. Phys. A 560 (1993) 633.
- [8] F. Androzzi, A. Covello, A. Gargano and A. Porrino, Phys. Rev. C 41 (1990) 250.
- [9] O. Scholten and H. Kruse, Phys. Lett. B 125 (1983) 113.
- [10] H. Sagawa, O. Scholten, B.A. Brown and B.H. Wildenthal, Nucl. Phys. A462 (1987) 1.
- [11] O. Scholten, H.C. Wu and A.E.L. Dieperink, Z. Phys. A 332 (1989) 1.
- [12] B.H. Wildenthal, Proc. of 3rd Int. Spring Seminar on Nuclear Physics, Ischia, Italy 1990, ed. A. Covello (World Scientific, Singapore, 1991) p. 35.
- [13] T. Engeland, M. Hjorth-Jensen, A. Holt and E. Osnes, Phys. Scripta T 56 (1995) 58.
- [14] T. Engeland, M. Hjorth-Jensen, A. Holt and E. Osnes, Proc. of the International Workshop on Double Beta Decay and Related Topics, ECT\*, Trento, Italy 1995, eds. H.V. Klapdor-Kleingrothaus and S. Stoica (World Scientific, Singapore, 1996) p. 421.
- [15] M. Hjorth-Jensen, T.T.S. Kuo and E. Osnes, Phys. Reports 261 (1995) 125.
- [16] T.T.S. Kuo and E. Osnes, Folded-Diagram Theory of the Effective Interaction in Atomic Nuclei, Springer Lecture Notes in Physics, (Springer, Berlin, 1990) Vol. 364.
- [17] K. Suzuki and R. Okamoto, Prog. Theor. Phys. 92 (1994) 1045.

- [18] K. Suzuki, R. Okamoto and H. Kumagai, Nucl. Phys. A 580 (1994) 213.
- [19] R. Machleidt, Adv. Nucl. Phys. 19 (1989) 189 .
- [20] C.A. Stone, J.D. Robertson, S.H. Faller, P.F. Mantica, B.E. Zimmerman, C. Chung and W.B. Walters, Phys. Scripta T56 (1995) 316.
- [21] R.R. Whitehead, A. Watt, B.J. Cole and I. Morrison, Adv. Nucl. Phys. 9 (1977) .
- [22] H. Grawe, R. Schubart, K.H. Maier, D. Seweryniak, the OSIRIS and NORDBALL collaborations, Phys. Scripta T 56 (1995) 71.
- [23] P. Kleinheinz, R. Broda, P.J. Daly, S. Lundari, M. Ogawa and J. Blomqvist, Z. Phys. A 290 (1979) 279.
- [24] M. Ogawa, R. Broda, P.J. Daly and P. Kleinheinz, Phys. Rev. Lett. 41 (1978) 289.
- [25] Y. Nagai, J. Styzen, M. Piiparinen, P. Kleinheinz, P. v. Brentano, K. Ozeth and J. Blomqvist, Phys. Rev. Lett. 47 (1981) 1259.
- [26] J. Suhonen, Nucl. Phys. A 563 (1993) 205.
- [27] A. Bohr and B.R. Mottelson, Nuclear Structure, vol. I (Benjamin, New York, 1963).
- [28] J. Suhonen and O. Civitarese, Nucl. Phys. A 584 (1995) 449.
- [29] M. Bertschy, S. Drissi, P.E. Garrett, J. Jolie, J. Kern, S.J. Mannanal, J.P. Vorlet, N. Warr and J. Suhonen, Phys. Rev. C 51 (1995) 103.
- [30] M. Baranger, Phys. Rev. 120 (1960) 957.
- [31] M. Grinberg, Thai Khac Dinh, Ch. Protochristov, I. Penev, C. Stoyanov and W. Andrejtscheff, J. Phys. G19 (1993) 1179.
- [32] B.H. Wildenthal, E. Newman and R.L. Auble, Phys. Rev. C 3 (1971) 1199.